Contrasting cloud properties in the trade wind region of Barbados in the dry and wet season

Roschke, J.[1], **Emmanouilidis, A.**[1]

[1] *Institut für Meteorologie, Stephanstraße 3, 04103 Leipzig,*
E-mail: jr55riqa@studserv.uni-leipzig.de,
E-mail: alexandros.emmanouilidis@uni-leipzig.de

Summary: A statistical analysis is provided in order to describe the macro- and microphysical properties of clouds over the Barbados. Data from the Cloudnet target classification product are analyzed for February and October 2013 and 2015 over the Barbados cloud observatory. The months February and October are taken to be representative for the dry and the wet season over Barbados. Hydrometeor fraction from the Cloudnet target classification and from a combination of cloud radar and ceilometer data are presented. Moreover, results of the distribution of the first layer of detected cloud base height from the ceilometer are presented. Additionally, the analysis for hydrometeor fraction and cloud base height are carried out for the measurements on board the Research Vessel Meteor during the EUREC^{4}A field campaign and compared to the observations over the Barbados cloud observatory in February 2020. The strongest seasonal variation of the vertical distribution of the Cloudnet classification targets appears between 3 and 9 km. The maximum occurrence of the first detected cloud base height is found at higher altitudes during the dry season compared to the wet season. The vertical distribution of hydrometeor fraction shows a bimodal distribution and is largest during the wet season. In general, the seasonal variation of the distribution of the Cloudnet targets, hydrometeor fraction and cloud base height between 0 and 3 km is less pronounced compared to heights above 3 km.

Zusammenfassung: Diese Studie enthält eine statistische Analyse der makro- und mikrophysikalischen Eigenschaften von Wolken über dem "Barbados Cloud Observatory". Es wurden Daten aus dem "Cloudnet target classification"-Produkt aus den Monaten Februar und Oktober für die Jahre 2013 und 2015 analysiert. Die Monate Februar und Oktober gelten als charakteristisch für die Trocken- und die Regenzeit. Der Hydrometeor-Anteil aus der Cloudnet Target Classification und aus der Kombination von Wolkenradar und Ceilometer-Daten wurden ermittelt. Die Verteilung der ersten Schicht der detektierten Wolkenbasishöhe aus den Ceilometer-Daten wurde abgeleitet. Zusätzlich wurden die Analysen für den Hydrometeor-Anteil und die Wolkenbasishöhe zwischen den Messungen an Bord des Forschungsschiffes Meteor während der EUREC^{4}A-Feldkampagne und den Beobachtungen über dem "Barbados Cloud Observatory" für Februar 2020 verglichen. Die Ergebnisse dieser Untersuchung zeigen, dass die stärkste saisonale Variation der vertikalen Verteilung des "Cloudnet target classification"-Produktes zwischen 3 und 9 km auftritt. Das maximale Auftreten der ersten detektierten Wolkenbasishöhe wird in der Trockenzeit in größeren Höhen gefunden als in der Regenzeit. Wolkenanteil und Hydrometeor-Anteil zeigen eine bimodale Verteilung und sind in

der Regenzeit am größten. Im Allgemeinen ist die saisonale Variation des Wolkenanteils, des Hydrometeor-Anteils und der Wolkenbasishöhe zwischen 0 und 3 km gering.

1 Introduction

Understanding patterns of cloudiness and advancing investigations of clouds are central to increase the confidence in fundamental aspects of climate change. However, much uncertainty still exists about the physical properties of clouds especially of those found within the trade wind regions (Stevens et al., 2016). Surveys such as that conducted by Medeiros and Nuijens (2016) have shown that clouds over Barbados are representative of clouds in the broader tropics. Thus, enhancing the knowledge about clouds over Barbados broadens the understanding of clouds within the trade wind region and improves their representation in climate models. A suitable location to observe clouds over Barbados is the Barbados Cloud Observatory (BCO), which is located on the island's eastern coast next to the Caribbean Sea. The observatory is equipped with ground-based remote sensing instruments that form the basis of Cloudnet (Stevens et al., 2016).
A statistical analysis of data from the Cloudnet target classification, cloud radar and ceilometer is presented to resolve the micro- and macrophysical properties of clouds over the BCO. In particular, the vertical distribution of Cloudnet classification targets, hydrometeor fraction (HF) and the first layer of the detected cloud base height (cbh^1) are compared from the dry to the wet season over Barbados. Finally, HF is compared between the instruments over the BCO and from the Research Vessel Meteor (R/V Meteor) during the EUREC^{4}A (Elucidating the role of clouds-circulation coupling in climate) field campaign, which took place in early 2020 (Bony et al., 2017).

2 Instrumentation and Methods

The data analyzed in this study are taken from the Cloudnet target classification, ground-based cloud-radar and ceilometer over the BCO. These data differ in their resolution and time period covered due to instrument exchanges. The years 2013 and 2015 were selected for the seasonal comparison out of the available Cloudnet data over the BCO (2011 until 2017) because they show the most continuous data coverage in February and October. Furthermore, an unrealistically high proportion of low clouds were misclassified as aerosols and insects by the Cloudnet algorithm in 2016. For this reason, the data from 2016 were not included in the analysis. Data from cloud radar and ceilometer are chosen for the same years. The months February and October are taken to be representative for the dry and the wet season as proposed from previous research by Stevens et al. (2016). Orientated on definitions provided by Stevens et al. (2016), low level clouds are defined as clouds located from 0 to 3 km. The mid-levels are defined as the height range from 3 to 9 km and the high-levels from 9 to 15 km. Heights below 1 km are referred to as near the lifting condensation level (near LCL). The methods used to derive HF and cbh^1 are based on studies of Stevens et al. (2016) and Nuijens et al. (2014). All data source and the methods that were applied to the data are described in the following sections.

2.1 Cloudnet data products

The Cloudnet project was started in 2001[1] in order to provide information about the physical state of the atmosphere from a synergy of ground-based remote sensing observations. The Cloudnet target classification product enables the identification of the physical phase of hydrometeors (Illingworth et al., 2007). Core instruments of a Cloudnet observation site are a cloud radar and a ceilometer. The measurements of these instruments are analyzed in combination with thermodynamic profiles of a model by the Cloudnet algorithms (Illingworth et al., 2007). In general, the ceilometer is used to identify the base of liquid water clouds. Liquid droplets are assigned when a threshold value is exceeded in the ceilometer signal followed by a characteristic decrease in signal above the cloud base. The cloud top is detecteed by the radar signal in case the ceilometer backscatter is not extinguished. Falling targets are assigned between cloud base and the highest pixel below cloud top when the radar signal decreases with height and the radar reflectivity exceeds −30 dBZ. Additionally, all radar echos in the profile are classified as falling in the case that rain is detected at the ground. Ice particles are assigned when falling targets are observed and the wet bulb temperature is below 0 °C. In the case that falling targets have been detected and additionally the wet bulb temperature is above 0 °C, the profile is categorized as containing precipitation. The height of the melting layer is derived either from the model data or when a sharp increase in the Doppler velocity is observed. A detailed description of the Cloudnet target classification algorithm can be found in Hogan and O'Connor (2004). An example of the Cloudnet classification product for the 25th of February 2015 is presented in Fig.1 (a) and after selecting the targets relevant for this study in (b). HF is calculated by taking the sum of all targets in each height bin (30 m).

In this study the original resolution of 30 m and 15 s is maintained. Profiles are analyzed for containing "Cloud droplets only", "Drizzle–rain and cloud droplets", "Ice and supercooled droplets", "Ice" and "Drizzle or rain." "Cloud droplets only" and "Drizzle-rain and cloud droplets" are combined to the category "Liquid droplets". The data from the Cloudnet target classification are processed with "pyLARDA", an algorithm designed by Bühl et al. (2018) simplifying the handling of the Cloudnet data.

2.2 Ceilometers

The Jenoptik CHM 15k(X) ceilometer measures at 1064 nm with a range resolution of 30 m and a temporal resolution of 30 s until April 2015 and 10 s since April 2015. The first cloudy point detected by the ceilometer is taken to be the cloud-base height (cbh^1). The ceilometer detects cbh^1 using a vertical gradient method explained in detail by Nuijens et al. (2014). A time range of 456 h was chosen to ensure an equal amount of data for the seasonal comparison. In this study, vertical profiles of cbh^1 are analyzed up to 4 km. Cloud-base height occurrence is derived by taking 50 m bins. Rain events are not excluded within the estimation of cloud base height. The ceilometer on board the R/V Meteor is a Jenoptik system ceilometer like over the BCO.

[1] https://cloudnet.fmi.fi

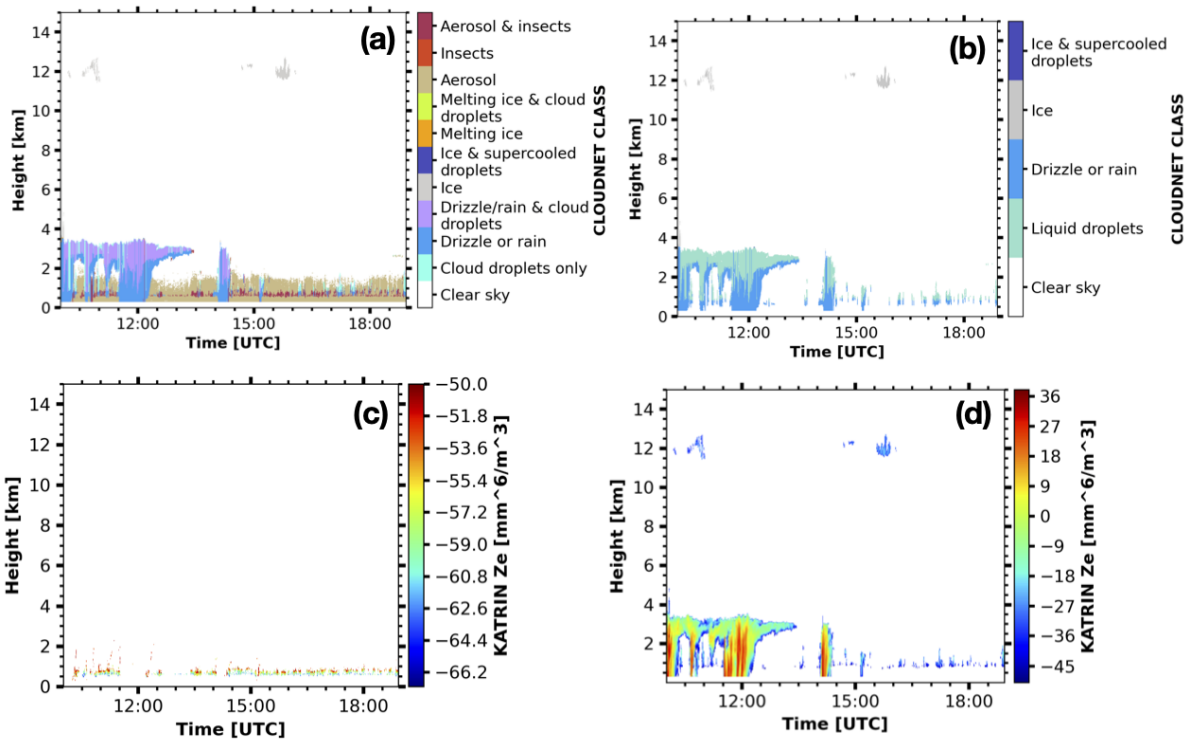

Figure 1: *The example output of the Cloudnet classification product over the BCO on the 25th of February 2015 is displayed. The unprocessed Cloudnet output (a) and the same scenario after selecting the relevant targets for the study in (b) are presented. The equivalent radar reflectivity* $-65\,\mathrm{dBZ} < Z_e < -50\,\mathrm{dBZ}$ *from KATRIN during the same time is displayed in (c) and with a threshold of* $-50\,\mathrm{dBZ}$ *in (d).*

2.3 Cloud radars

The cloud radars KATRIN and CORAL from the BCO operate at 35.5 GHz. KATRIN was replaced by CORAL in April 2015 which is still ongoing. Profiles from KATRIN are taken every 30 s with a range resolution of 30 m. Since KATRIN operated from January 2011 to mid-May 2011 and October 2011 in an alternating vertical pointing and scanning mode, the data from 2011 is excluded from the analysis (Nuijens et al., 2014). CORAL measures with a resolution of 10 s and 30 m. Additionally, data from the RPG 94 GHz polarized cloud radar LIMRAD94 on board the R/V Meteor were analyzed.
Hydrometeor fraction is estimated by combining radar and ceilometer data as proposed by Bony et al. (2017). All radar signals detected above the cbh^1 account for the hydrometeor fraction. Due to differences in the instrument resolutions, the data is averaged with a temporal resolution of 30 s and spacial resolution of 30 m as displayed in Fig.2. Each radar signal where the equivalent radar reflectivity Z_e exceeds $-50\,\mathrm{dBZ}$ is defined as a true hydrometeor return as proposed by Klingebiel et al. (2019) to ensure that haze echos are excluded. Comparing Fig.1 (a) and (c), weak radar signals between $-65\,\mathrm{dBZ} < Z_e < -50\,\mathrm{dBZ}$ are classified as "Aerosols and insects" by the Cloudnet algorithm and are excluded in the analysis. Following methods from previous research by Nuijens et al. (2015a) all returns below cbh^1 indicating drizzle are excluded.
An example of hourly mean HF resolved for each season in 2015 can be seen in Fig.7. The vertical distribution of monthly mean HF is presented for the dry and the wet season

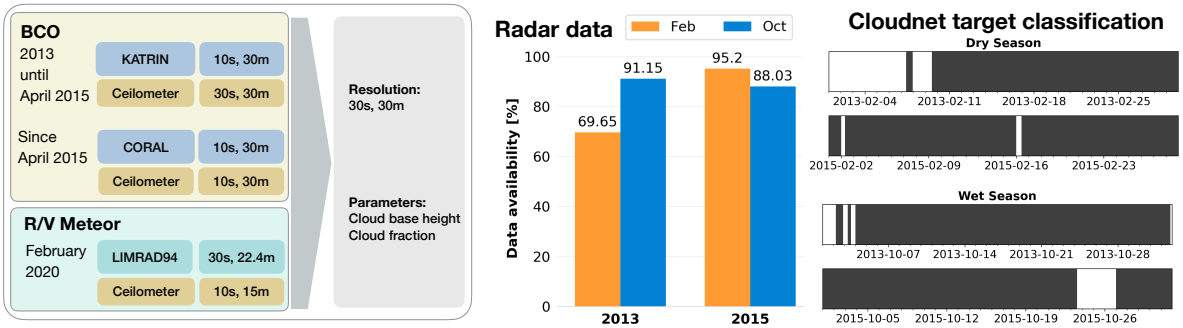

Figure 2: *Resolution and data availability of the relevant instruments used to derive cloud fraction and cloud base height at the BCO and R/V Meteor. The data from the different instruments are averaged on a common grid with a resolution of* 30 s *and* 30 m. *The radar data availability at the BCO is presented on the right for February and October in 2013 and 2015.*

in 2015 (the original resolution was maintained). For the statistics no data are excluded even though the radar data coverage is not equal every time. Interpretations of monthly mean HF have to be made under consideration of this fact.

3 The vertical distribution of cloud

A statistical analysis of the vertical distribution of the targets from the Cloudnet data, cbh[1] and HF from the Cloudnet data and from the combination of radar and ceilometer data are presented. The method deriving HF is applied on the measurements on board the R/V Meteor and compared to the observations over the BCO in February 2020.

3.1 Cloudnet target classification

Cloudnet target classification distributions are shown in Fig.3 partitioned into Liquid droplets (1), Drizzle or rain (2), Ice (3) and Ice and supercooled droplets (4) for the dry and the wet season. Liquid droplets (1) occurred more frequent at 780 m (8.8 %) during the dry season compared to the wet season at 750 m (7.2 %) . This supports findings of Nuijens et al. (2014) who pointed out that clouds start to form in higher altitudes during the dry season compared to the wet season. Liquid droplets (1) show a second peak at 1.8 km during the dry season and a weaker peak at 1.5 km during the wet season, potentially indicating deeper and more developed cumuli with stratiform outflow. Nuijens et al. (2014) also assigned the second peak in profile of HF to stratiform cloud layers which are located close to the trade inversion. Also, these results seem to be consistent with research from Lamer et al. (2015) who point out a higher occurrence of stratiform layers during the dry season and a considerable absence of precipitating boundary layer clouds during the wet season in 2013 over the BCO.
Drizzle or rain (2) occurred most often at 540 m during both seasons. Consequently, a noticeable amount of Drizzle or rain (2) during the dry season can be contributed to be originated from shallow cumuli and those with stratiform like outflow. This also supports evidence from previous observations such as Nuijens et al. (2009), Vogel et al. (2016),

Rauber et al. (2007) and Short and Nakamura (2000) who showed that precipitation from shallow cumulus occurs often. Short and Nakamura (2000) also mentioned that the intensity of warm rain from shallow clouds increases as they grow deeper and that shallow cumulus producing rainfall typically extend up to 2 km. Accordingly, it can be assumed that a high proportion of the precipitation was caused by clouds contributing to the maximum in Liquid droplets (1) in 1.8 km.

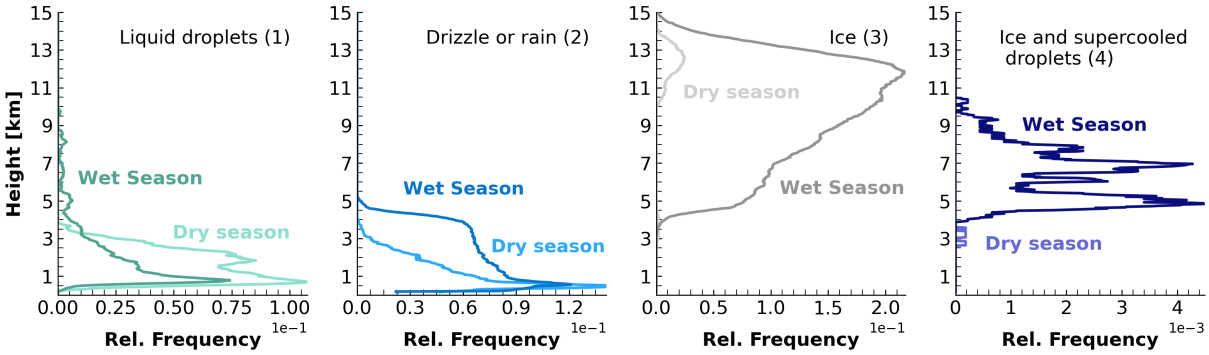

Figure 3: *Relative Frequencies of Cloudnet target classification for the targets Liquid droplets (1) , Drizzle or rain (2), Ice (3), and Ice and supercooled droplets (4) during dry and wet season. Data for dry and wet season are summed up for February and October (2013 and 2015) respectively.*

Ice (3) in Fig.3 showing a higher occurrence during the wet season compared to the dry season. Indeed, the occurrence of cirrus clouds is related to the presence of deep convective clouds which dominate during the wet season as mentioned by Sassen et al. (2009). The sharp decrease in Ice (3) occurrence below 5 km marks the average height at which ice starts to melt during the wet season, also indicated by the minimum in the distribution of HF in Fig.6 (a) at 4.3 km (Melting ice from the original Cloudnet target classification is excluded in the analysis). Short and Nakamura (2000) refers to the influence of the melting level on the statistics of the storm height. Accordingly, the 0 °C isotherm is located at an average height of 5 km in the tropics. Melting ice, which appears as an area of increased reflectivity in the radar signal below 0 °C isotherm was not included in the statistics and therefore appears as a minimum in the vertical distribution of HF.
Ice and supercooled droplets (4) were rarely observed compared to the other Cloudnet targets but significantly more frequent during the wet season compared to the dry season. Moreover, the distribution of Ice and supercooled droplets (4) indicates, that mixed phase clouds containing combination of the targets (1), (3) and (4) were more frequent during the wet season.

An overview of the height ranges at which the respective targets occurs mostly in relation to each other is presented in Fig.4. The monthly target proportion corresponds to the mean frequency of occurrence (for the height ranges near LCL, low, mid, high and total) of all targets shown in Fig.4. The results show that only Liquid droplets (1) and Drizzle or rain (2) are present near the LCL and within low levels during both seasons. The proportion of Drizzle or rain (2) increases during the wet season near the LCL and in the low levels. Concluding from this, the total observed precipitation must not only result from clouds in the low levels but also from deep convective clouds which increase the

frequency of occurrence of Drizzle or rain (2) above and below 3 km during the wet season.
What stands out is that the highest seasonal variation of the target proportions occurs within the mid-levels. The ratio change can be explained by the increase in total target occurrence mainly due to the increase in Ice (3) occurrence during the wet season. Moreover, the ratio of Liquid droplets (1) to Drizzle or rain (2) changes with the former dominating in the dry season and the latter dominating over Liquid droplets (1) during the wet season. The targets Liquid droplets (1) and Drizzle or rain (2) dominate over Ice (3) and Ice and supercooled droplets (4) over the total height range during the dry season. Moreover, the target proportion changes during the wet season with Ice (3) dominating because of deep convective clouds which are more commonly observed during the wet season as the comparison in 7 indicates.. The ratio of Drizzle or rain (2) to Liquid droplets (1) changes with (2) being greater than (1) during the wet season.

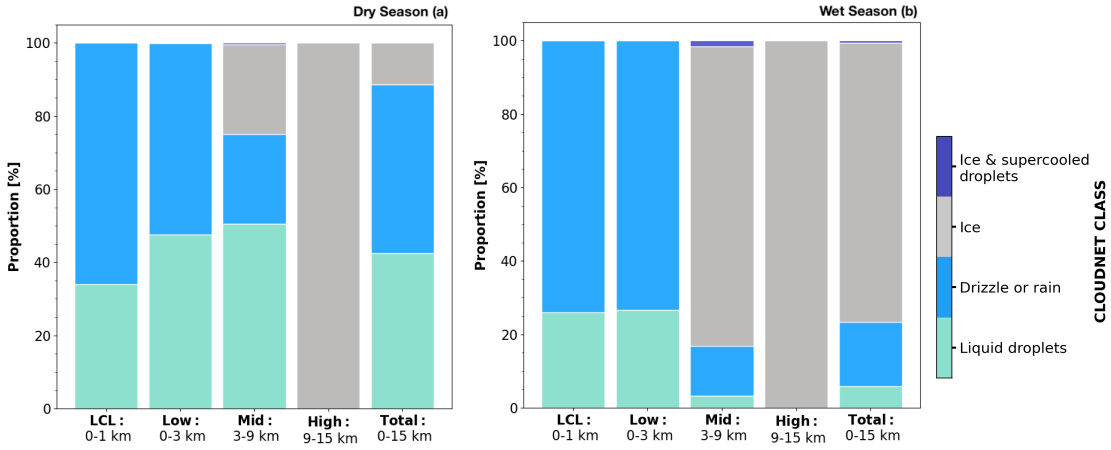

Figure 4: *Proportion of Cloudnet classification targets relative to each other for different height ranges for the dry (a) and wet (b) season.*

3.2 Cloud-base height distribution

The maximum occurrence in cbh^1 detected by the ceilometer in Fig. 5 is located below the LCL (<1 km). During the dry season this peak is found at 746±100 m and during the wet season at 646±100 m. The peak during the dry season is located at a similar height compared to the maxima in Liquid droplet (1) occurrence. However, the results from the Cloudnet target classification indicate that low level liquid clouds are more frequent during the dry season compared to the wet season which seems to be contradictory to the findings in cbh^1 occurrence showing larger frequencies during the wet season. The higher occurrence in cbh^1 during the wet season detected by the ceilometer is suggested to be overestimated due to heavier rain events during the wet season which can distort the ceilometer signal (Nuijens et al., 2014). Compared to the dry season, the results of cbh^1 from the ceilometer correspond more with the Cloudnet target classification results despite precipitating targets (Drizzle or rain (2)) being frequently observed. However, the ceilometer is able to detect cbh^1 during light rain events which are suggested to be occurred more often during the dry season. Consequently, the results in cloud base height are less accurate during the wet season compared to the dry season. However, the

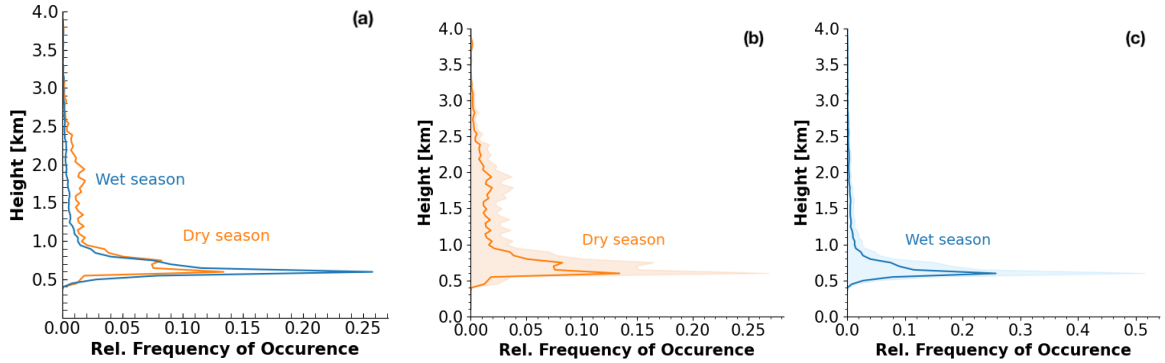

Figure 5: *Relative frequency of occurrence of cloud base height (*50 m *bins) provided by the ceilometer over the BCO (a) with shaded areas showing the standard deviation for each distribution during the dry (b) and wet (c) season.*

spread in height between the two peaks reflects the range in LCL from the dry to the wet season as indicated in the previous section. Clouds start to form at higher altitudes during the dry season compared to the wet season. Thus, the bases of clouds during the dry season are located higher up (Nuijens et al., 2015b). cbh^1 becomes less frequent above 1 km with the hint of a second maximum between 1 and 1.5 km which might reflect the presence of clouds with stratiform outflows (Nuijens et al., 2015b). Above 1.5 km cbh^1 is becoming less frequent which confirms findings presented by Nuijens et al. (2014) and Nuijens et al. (2015b).

3.3 Cloud fraction

Fig. 6 (a) represents the HF estimated from the Cloudnet target classification by taking the sum over the four targets presented within this study. In general, the occurrence of low level clouds is less variable during the seasons compared to mid and high levels. Total HF is larger during the wet season compared to the dry season with the seasonal variability being more pronounced on mid and high levels. The vertical distribution of HF in (a) and (b) is bimodal in both seasons which confirms earlier findings by Stevens et al. (2016). The seasonality of clouds over the BCO is related to the migration of the ITCZ which produces circulation shifts and large changes in cloudiness (Stevens et al., 2016). Large scale subsidence during the dry season suppresses the development of deeper clouds which explains why mid and high level clouds are less frequent during the dry season. The higher frequency of clouds in the mid and high levels during the wet season is caused by upward motion that favors the formation of deep convective clouds (Nuijens et al., 2015a). Furthermore, the atmosphere is more humid through a deeper layer during the wet season which is why HF is on average higher.
The low level total HF occurrence from the Cloudnet data shows a peak at 630 m (21 %) during the dry season which indicates the presence of Drizzle or rain (2) as described in the previous section. Findings by Nuijens et al. (2015a) suggest that the cloud base is located where the profile in low levels of HF maximizes. This idea is supported in the second peak at 840 m (19 %) during the dry season and at 750 m (17 %) during the wet season which are located at a similar height as most cloud bases and also of the maximum occurrence of Liquid droplets (1). Thus, it is suggested that these peaks reflect

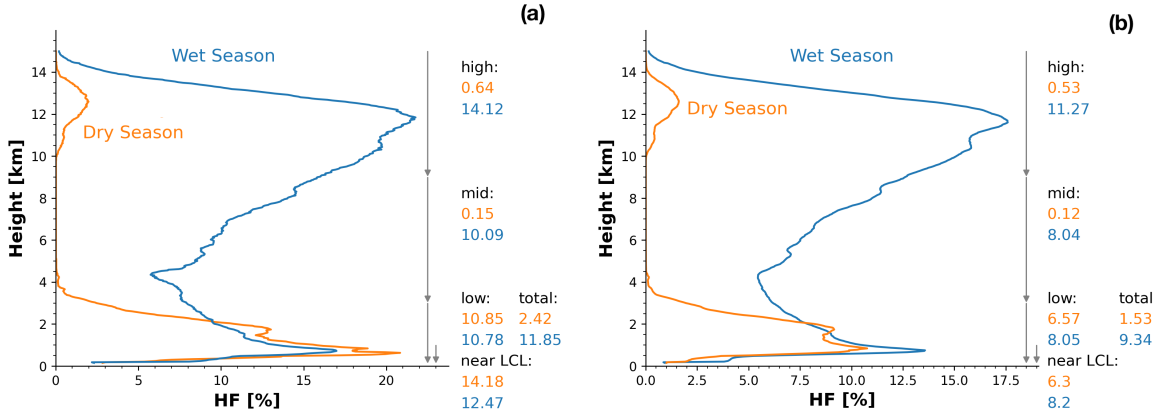

Figure 6: *Vertical profiles of hourly mean hydrometeor fraction (HF) from the Cloudnet target classification (a) and derived combining cloud radar and ceilometer data (rain is not excluded) (b). Means over the height levels (near LCL: 0-*1 km*, low: 0-*3 km*, mid: 3-*9 km*, high: 9-*15 km*, total: 0-*15 km*) during both seasons are presented.*

shallow clouds rather than Drizzle or rain (2). The first maximum in Fig.6 b is found at the same height during the dry season but with a smaller occurrence in HF (11 %). The lower occurrence in Fig. 6b must result from the chosen threshold in the radar return. Lowering the threshold would include more optically thin clouds or drizzle that is falling from cloud bases and evaporates in the sub-cloud layer. Consequently, lowering the threshold would result in larger frequencies of HF in the low levels as indicated by Nuijens et al. (2014). Moreover, Nuijens et al. (2015a) suggest that the first low level peak in HF is related to the presence of shallower trade-cumuli. On average, the peak within the low levels during the wet season is located at smaller altitudes because of higher relative humidity in the atmosphere. This influences the cloud formation process to start at lower altitudes (lower LCL) during the wet season than during the dry season. Also, rain events that were not filtered out and are more common during the wet season might have led to an overestimation of HF (Nuijens et al., 2015a).
In comparison to the changes in HF through all height levels, HF does not vary much at low levels from the dry to the wet season supporting the findings by Stevens et al. (2016). The second peak during the dry season in Fig. 6b is located at 1.7 km with an occurrence of 9 % corresponding to the height were the second peak in low level Liquid droplets (1) and cbh^1 is found. Also the hint of this second maximum can be seen in the distribution of HF during the wet season. This supports the theory of Nuijens et al. (2015a) who pointed out that deeper cumulus clouds with tops near the trade inversion are common during the dry season. Furthermore, it is assumed by Nuijens et al. (2015a) that deep convective cloud systems suppress cloud formation in their near surroundings during the wet season. As a result, deep convective clouds are less frequently surrounded by smaller cumuli near the trade inversion during the wet season (Nuijens et al., 2015a). HF decreases through the mid-levels during the dry season showing a second peak in high levels during the dry season which reflects high level cirrus clouds. HF during the wet season decreases from a second maximum near the LCL through the mid-levels and increases with height above 4.2 km were the average melting layer was indicated as in previous results in the distribution of the Cloudnet targets.

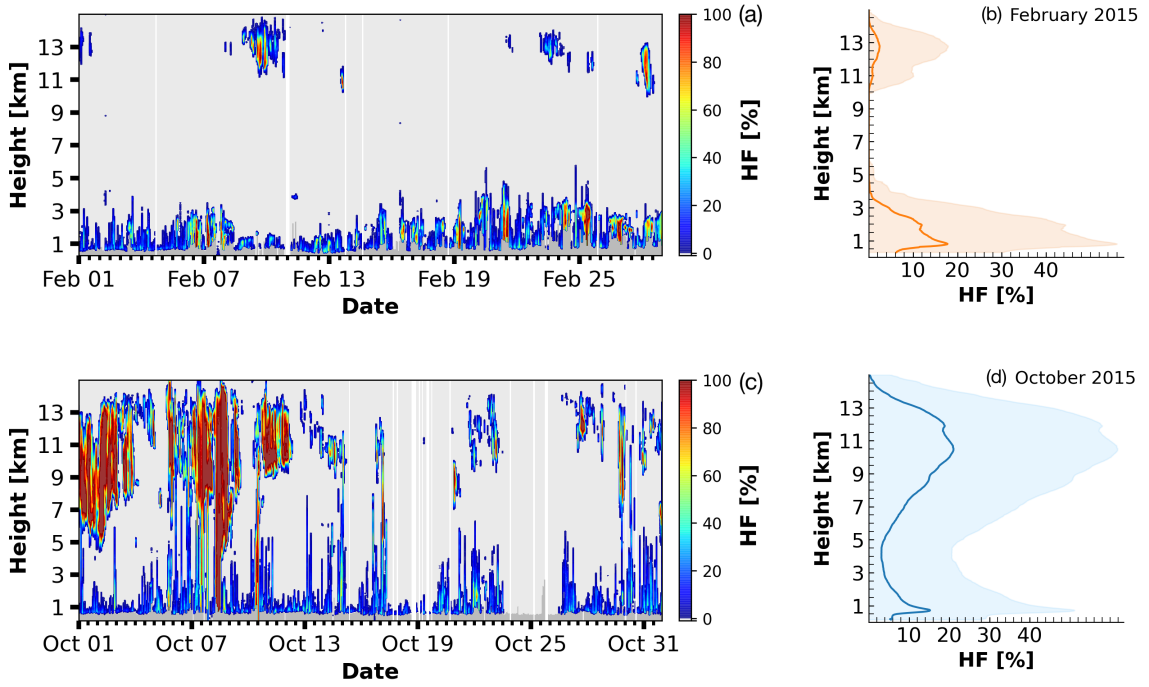

Figure 7: *Vertical profile of hourly mean hydrometeor fraction (HF) derived by combining CORAL Cloud radar and ceilometer data for February (dry season) (a) and October (wet season) (c) 2015 over the BCO. Note that white bars occur when data gaps are present and grey corresponds to clear sky. Vertical profile of monthly mean cloud fraction (the original resolution is maintained) for the dry (b) and wet season (d) in 2015 over the BCO with the estimated standard deviation.*

As an example of the distribution of clouds over a month hourly mean HF (taken to increase the readability of the figure) are presented in Fig. 7 for February and October 2015 (representative for dry and wet season). Deep convective clouds can be seen especially during the first half of the month in October. Furthermore, it can be seen that the distribution of low clouds does not change much over the dry and wet seasons. However, during the dry season, more low-level clouds with increased HF are evident, especially in the second half of the month. Additionally to the previous results, this indicates that deeper clouds are more common during the dry season than during the wet season.

Fig. 8 provides an overview about the distribution of monthly mean HF during February 2020 on board the R/V Meteor and the BCO. Averaged hourly HF do not reflect the distribution over the BCO typical during the dry season which is due to the maximum in HF in the mid-levels, which appears to be uncharacteristic for the dry season in comparison to previous findings over the BCO. This is suggested to be caused by the amount of data which is included in the analysis. Moreover, the increase in HF within the mid-levels can be attributed to the event between the 14th and 17th February. The first maximum is located at 872 m in the low levels with a lower frequency than the second one at 1.7 km above the R/V Meteor. Over the BCO, the first maximum is located in 811 m and the second one at the same altitude as above the R/V Meteor. The second

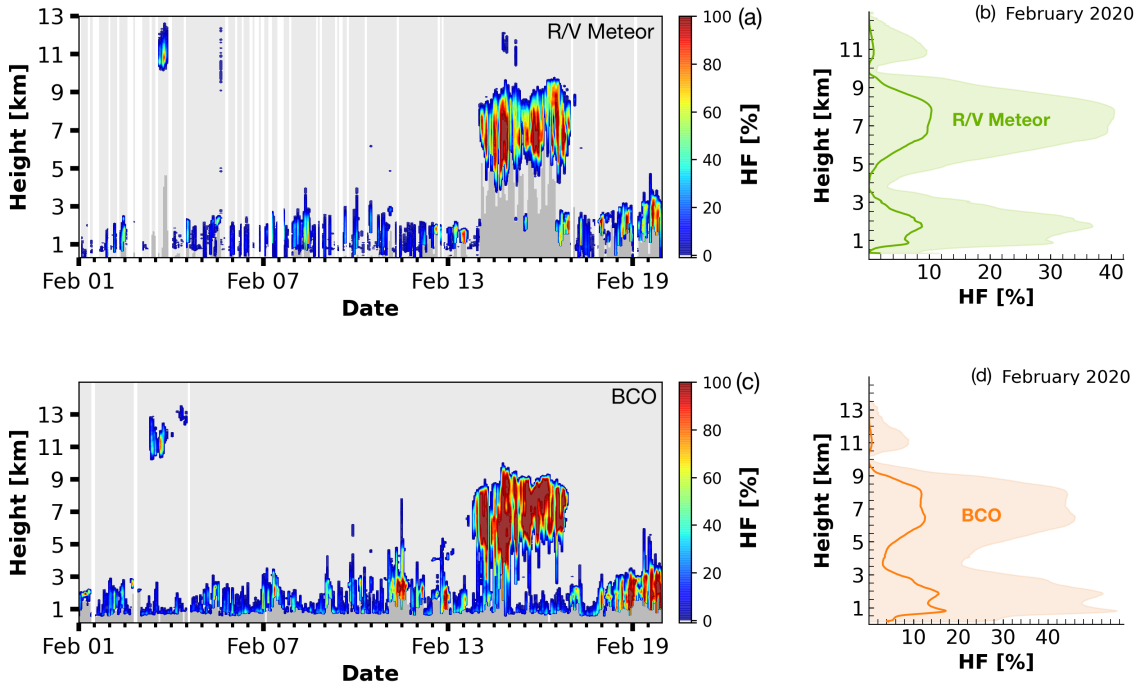

Figure 8: *Vertical profile of hourly mean hydrometeor fraction (HF) in February 2020 on board the R/V Meteor (a) and over the BCO (c). Note that white bars occur when data gaps are present and grey corresponds to clear sky. Vertical profile of mean hydrometeor fraction (original resolution maintained) over the BCO (b) and on board the R/V Meteor (d) with the estimated standard deviation.*

peak over the BCO is more than twice as compared to the low level maximum from the R/V Meteor. An explanation might be the difference in the radars operating on 94 GHz (with corresponding wavelength 3.2 mm) over the R/V Meteor and on 35.5 GHz (with corresponding wavelength 8.6 mm) over the BCO. The signal on smaller wavelengths is more attenuated by large hydrometeors like drizzle or rain compared to measurements on larger wavelengths (Görsdorf et al., 2015). Consequently, the radar over the R/V Meteor misses larger particles located below the cloud bases and shallow cumuli located near the LCL. Thus, it might be possible that the 94 GHz radar underestimates HF near the LCL. In contrast, the radar over the BCO successfully detects large liquid droplets or drizzle located near the LCL which explains the higher occurrence in HF on these levels.

4 Conclusions & Outlook

This work contributes to existing knowledge of clouds in the trade wind region by providing insights into the distribution of macro- and microphysical properties of clouds over the Barbados cloud observatory (BCO). Data from February were taken to be representative for the dry season and data from October for the wet season. The present study is one of the first attempts to examine the micro- and macro-physical properties of clouds from the Cloudnet target classification product over the BCO. Two years (2013 and 2015) were analyzed from a seven year data set of the Cloudnet target classification product to resolve the vertical distribution of cloud properties. The chosen Cloudnet targets are Liquid Droplets (1), Drizzle or rain (2), Ice (3) and Ice and supercooled droplets (4). HF was estimated combining cloud radar (Ka-band, KATRIN and CORAL) and ceilometer data from the BCO. A comparison of HF estimated from the Cloudnet data and the combination from radar and ceilometer data from the BCO were carried out. Furthermore HF was estimated combining cloud radar (W-band cloud radar LIMRAD94) and ceilometer data on board the R/V Meteor and over the BCO for the dry season in February 2020.

The results of this investigation show that the strongest seasonal variation of the Cloudnet classification targets appears on the mid-levels. While Liquid droplets (1) dominate during the dry season, the proportion of Ice (3) is significantly increased on the mid-levels during the wet season. The proportion of Liquid droplets (1) also decreases during the wet season in the mid-levels. Low clouds show little variability over the BCO, which is supported in the vertical distributions of Liquid Droplets (1) and Drizzle or rain (2) that do not change much from the dry to the wet season. The occurrence in Drizzle or rain (1) shows that precipitation originating from low clouds appears with nearly the same frequency over the seasons. However, the proportion of Drizzle or rain (2) increases during the wet season as precipitation from deep convective clouds contributes to an increase in the distribution of HF within the mid-levels.
The maximum occurrence of cbh^1 during the dry season at 746±100 m is found at higher altitudes compared to the wet season at 646±100 m. The maxima in HF at the lower levels, indicating the presence of shallow cumuli, are located at 840 m altitude during the dry season and at 750 m altitude during the wet season. The differences compared to the results in cbh^1 can be related to difference in the ceilometer sensitivity thresholds which determine how many thin clouds near cbh^1 are detected (Nuijens et al., 2009). Moreover, different range resolutions also influence the distribution of the low level maxima. Thereby, 50 m bins were chosen in the statistics for cbh^1 and the height resolution in the calculations for HF of 30 m was maintained.
HF shows a bimodal distribution and is overall largest during the wet season over the BCO. The highest seasonal variation appears within the mid and high levels. On the low levels HF does not vary much over the seasons. The second peak in HF is located near the trade inversion at 1.7 km and is more pronounced during the dry season compared to the wet season. Additionally, the results of cbh^1 show a second maximum located at 1.5 km which is linked to the presence of more developed cumuli with stratiform outflow. Deep convective clouds occur often during the wet season, which, according to Nuijens et al. (2014), suppress cumuli near the trade inversion between 1.5 and 2 km.

The transferability of these results is subject to certain limitations. For instance, the statistics were qualified by the available data. Each year displays data gaps during different times of the months. Taking more data into account would result in more accurate statistics and profiles of all variables and targets. Besides the gaps in data availability, the estimation of HF was mainly aggravated by varying instrument settings of the ceilometer and the exchange of the radar in April 2015. Due to that, the data had to be interpolated on a common range and time resolution. Moreover, the distribution of HF

is influenced by the chosen threshold of the radar and the ceilometer. A lower threshold in the radar will include smaller particles and will mostly influence the distribution of HF on the low levels. By comparing findings from the BCO to the findings from the R/V Meteor it has to be considered that the radars operate at different sensitivities (94 GHz for the R/V Meteor and 35.5 GHz over the BCO). Consequently, the radar on board the R/V Meteor underestimates the amount of low level clouds in comparison to the radar operating at the BCO. Another source of uncertainty is that rain was not filtered out within the procedure. The instruments do not provide accurate information when rain is present. Results from Nuijens et al. (2014) indicate that including rain increases the distribution of HF at most levels but do not change the shape of the cloud profile and its variability with time. Furthermore, the classification of hydrometeors in Cloudnet can lead to erroneous profiles in liquid water if the radar signal is dominated by larger particles like rain and the ceilometer signal is attenuated (Hogan and O'Connor, 2004). Also, an unusually high occurrence of aerosols and insects was observed in the Cloudnet data in 2016. In this case, most shallow cumuli were misclassified as aerosols and insects. The misclassification is likely related to a weak signal from the ceilometer and a missing radar signal necessary to detect falling particles and liquid water droplets.

Despite these promising results, questions remain and ideas advancing future work emerged. First of all the statistics could be improved by implementing more data. The ceilometer at the BCO measured almost continuously. Time series and long term means of cbh[1] could contribute to confirm previous findings. Other variables such as cloud cover which is a popular derived parameter in studies could be statistically analyzed and compared to previous work. Furthermore, profiles of humidity, temperature and other meteorological parameters could help describing the environment as they influence cloud formation and development. It could be tested if the time period of the investigation was representative for the climate over Barbados or explains the occurrence of unusual events. In addition, the frequency of occurrence of different hydrometeors as a function of the temperature and humidity observed inside clouds could improve the representation of microphysical properties and their dependency on temperature and humidity. Moreover, the Cloudnet target classification product provides more parameters like liquid water content, ice water content and effective radius of the detected particles which are important properties to describe cloud properties. Era interim data could resolve the seasonal cycle by providing the parameter vertical pressure velocity. This parameter shows at what time of the year the dry or wet season appears. On that basis, data from more months could be included to the respective season and in return more accurate statistics could be realized. Data from a micro rain radiometer could help to exclude rain events. Furthermore, a micro rain radiometer is a commonly used instrument in combination with radar and ceilometer data to derive cloud fraction as conducted in previous studies by Nuijens et al. (2014). An equal combination of instruments in deriving parameters such as cloud fraction would assist to make the results more comparable to previous findings over the BCO.

All in all, this study might advance future investigations and either improve existing methods or help to improve instrument settings resolving the vertical distribution of clouds. In return, this will help to produce more accurate parameterization schemes of clouds in climate models. As clouds contribute to the largest uncertainties in climate sensitivity, it is necessary to support further investigations to expand data sets of meteorological parameters and to improve forecast models.

References

Bony, S., Stevens, B., Ament, F., et al.: EUREC 4 A: a field campaign to elucidate the couplings between clouds, convection and circulation, Surveys in Geophysics, 38, 1529–1568, 2017.

Bühl, J., Radenz, M., Schimmel, W., and Vogl, T.: pyLARDA, URL `https://lacros-tropos.github.io/larda-doc/html/index.html#`, 2018.

Görsdorf, U., Lehmann, V., Bauer-Pfundstein, M., et al.: A 35-GHz polarimetric Doppler radar for long-term observations of cloud parameters—Description of system and data processing, Journal of Atmospheric and Oceanic Technology, 32, 675–690, 2015.

Hogan, R. J. and O'Connor, E. J.: Facilitating cloud radar and lidar algorithms: the Cloudnet Instrument Synergy/Target Categorization product, Cloudnet documentation, 2004.

Illingworth, A., Hogan, R., O'connor, E., et al.: Cloudnet: Continuous evaluation of cloud profiles in seven operational models using ground-based observations, Bulletin of the American Meteorological Society, 88, 883–898, 2007.

Klingebiel, M., Ghate, V. P., Naumann, A. K., et al.: Remote sensing of sea salt aerosol below trade wind clouds, Journal of the Atmospheric Sciences, 76, 1189–1202, 2019.

Lamer, K., Kollias, P., and Nuijens, L.: Observations of the variability of shallow trade wind cumulus cloudiness and mass flux, Journal of Geophysical Research: Atmospheres, 120, 6161–6178, 2015.

Medeiros, B. and Nuijens, L.: Clouds at Barbados are representative of clouds across the trade wind regions in observations and climate models, Proceedings of the National Academy of Sciences, 113, E3062–E3070, 2016.

Nuijens, L., Stevens, B., and Siebesma, A. P.: The environment of precipitating shallow cumulus convection, Journal of the Atmospheric Sciences, 66, 1962–1979, 2009.

Nuijens, L., Serikov, I., Hirsch, L., Lonitz, K., and Stevens, B.: The distribution and variability of low-level cloud in the North Atlantic trades, Quarterly Journal of the Royal Meteorological Society, 140, 2364–2374, 2014.

Nuijens, L., Medeiros, B., Sandu, I., and Ahlgrimm, M.: The behavior of trade-wind cloudiness in observations and models: The major cloud components and their variability, Journal of Advances in Modeling Earth Systems, 7, 600–616, 2015a.

Nuijens, L., Medeiros, B., Sandu, I., and Ahlgrimm, M.: Observed and modeled patterns of covariability between low-level cloudiness and the structure of the trade-wind layer, Journal of Advances in Modeling Earth Systems, 7, 1741–1764, 2015b.

Rauber, R. M., Stevens, B., Ochs III, H. T., et al.: Rain in shallow cumulus over the ocean: The RICO campaign, Bulletin of the American Meteorological Society, 88, 1912–1928, 2007.

Sassen, K., Wang, Z., and Liu, D.: Cirrus clouds and deep convection in the tropics: Insights from CALIPSO and CloudSat, Journal of Geophysical Research: Atmospheres, 114, 2009.

Short, D. A. and Nakamura, K.: TRMM radar observations of shallow precipitation over the tropical oceans, Journal of Climate, 13, 4107–4124, 2000.

Stevens, B., Farrell, D., Hirsch, L., et al.: The Barbados Cloud Observatory: Anchoring investigations of clouds and circulation on the edge of the ITCZ, Bulletin of the American Meteorological Society, 97, 787–801, 2016.

Vogel, R., Nuijens, L., and Stevens, B.: The role of precipitation and spatial organization in the response of trade-wind clouds to warming, Journal of Advances in Modeling Earth Systems, 8, 843–862, 2016.